Electronic Supplementary Material (ESI) for RSC Advances.

Electronic Supplementary Information

Protein-activated transformation of silver nanoparticle into blue and red-emitting nanoclusters

*Dillip Kumar Sahu, Priyanka Sarkar, Debabrata Singha and Kalyanasis Sahu**

Department of Chemistry, Indian Institute of Technology Guwahati, Guwahati 781039, Assam, India

*E-mail: ksahu@iitg.ernet.in

Contents

Experimental section

Figure S1. Stability of AgNPs-BSA at neutral pH.

Figure S2. TEM image of AgNP taken after 10 min of the pH jump by NaOH treatment.

Figure S3. Effect of $NaBH_4$ on the dissolution of BSA-AgNPs.

Figure S4. Excitation spectra of blue and red AgNCs obtained from various routes.

Figure S5. pH jump experiment of citrate-capped AgNPs

Figure S6. Fluorescence decays of red-emitting Ag_{13}NCs obtained from different routes.

Table S1. Decay parameters of red-emitting Ag_{13}NCs obtained from different routes.

Figure S7. Fluorescence decays of blue-emitting Ag_8NCs obtained from different routes.

Table S2. Fluorescence decay parameters of blue-emitting Ag_8NCs obtained from different routes.

Figure S8. Stability of Ag_{13}NCs and Ag_8NCs stored at a low temperature (4 °C)

Figure S9. Emission spectra of red AgNCs at low temperature and low pH (pH 6).

Figure S10. Dissolution kinetics of AgNP initiated by pH jump to 11.5 by addition of NaOH.

Figure S11. Circular dichroism spectra of native BSA, BSA-AgNP, BSA-capped blue and red-emitting clusters.

Table S3. The secondary structure parameters of the BSA protein (□ helix, □ sheet and random coil percentage) at various conditions.

Experimental Section

Materials used. Silver nitrate (99.9999 %), bovine serum albumin and human serum albumin were purchased from sigma Aldrich. Sodium hydroxide and sodium borohydride were obtained from Merck chemicals. Ultrapure Milli-Q deionized water (18.2 MΩ) was used in all experiments.

Instruments and Methods. UV-visible absorption spectra were recorded in a Perkin-Elmer lamda750 spectrophotometer using a short path length cuvette of 0.1 cm. For steady state fluorescence, Jobin-Yvon FluoroMax4 was used with a 3 mm path length cuvette. Quantum yields (QY) were calculated with fluorescein in ethanol as a reference (QY 79%).[33] Matrix assisted laser desorption ionization (MALDI) mass spectra were measured in a Bruker MALDI-TOF spectrometer equipped with a 355 nm nitrogen pulse laser. Sinapinic acid was used as matrix for MALDI mass sample preparation. Fluorescence decays were collected in a time-correlated single photon counting (TCSPC) set up from Horiba instruments using a 375 nm laser diode. The images of the nanomaterials were taken through carried out in JEOL JEM 2100F transmission electron microscope (TEM) operating at 200 kV. Image-J software was used to analyze the size distribution of the nanomaterials considering the sizes of at least 50 particles. Circular dichroism (CD) spectra were obtained in a JASCO-1500 instrument with a path length of 1 mm. The CD spectra were analyzed through CDSSTR algorithm in Dicroweb software.

Preparation of BSA-capped AgNPs. The BSA-AgNPs were synthesized following an earlier report of Gebregeorgis et al. with slight modified.[24] 2 ml of 10 mM $AgNO_3$ solution was added dropwise to 2 ml of BSA (50 mg/ml) under 1200 rpm stirring at 37 °C. To this solution, an optimized amount (200 µl) of 10 mM $NaBH_4$ was gradually added and stirred for ~15 mins. A brown color was locally developed upon the addition of each drop of $NaBH_4$ and finally, the whole solution turned into dark brown. The pH of the resulting solution was found to be 6.

Transformation of AgNPs to blue-emitting AgNCs. 80 µl of 1 M NaOH solution was added to the BSA-capped AgNP solution to adjust the pH of the solution to 11.50. The initial dark brown color of the AgNP solution was faded to light brown within first 2 hours and gradually changes to

light yellow color after a waiting period of ~9 days. Absorption and fluorescence of the solution was measured from time to time to monitor the transformation. The solution was stirred continuously with a magnetic stirrer at 1200 rpm maintaining the temperature at 37 °C.

Transformation from red-emitting to blue-emitting AgNCs. First, pH of the BSA-capped AgNP was adjusted to 11.50 following the above procedure. After a delay of ~10 mins, 50 µl of 10 mM $NaBH_4$ was added and stirred for ~1 hour with a stirring speed of 1200 rpm at 37 ºC. The dark brown color of AgNPs turns to brown within 1 hour. The solution is stable at low temperature (4 ºC) or on acidification with HNO_3.

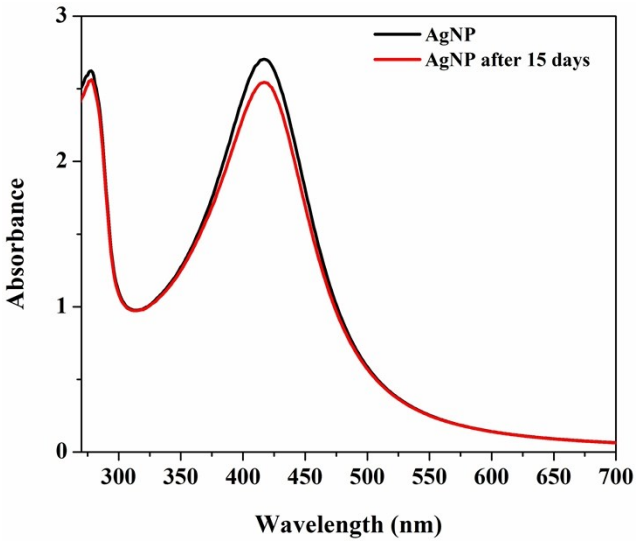

Figure S1. UV-Vis spectra of fresh BSA-capped AgNPs and after 15 days at pH = 6. No appreciable change of the spectra indicates high stability of nanoparticles at this condition.

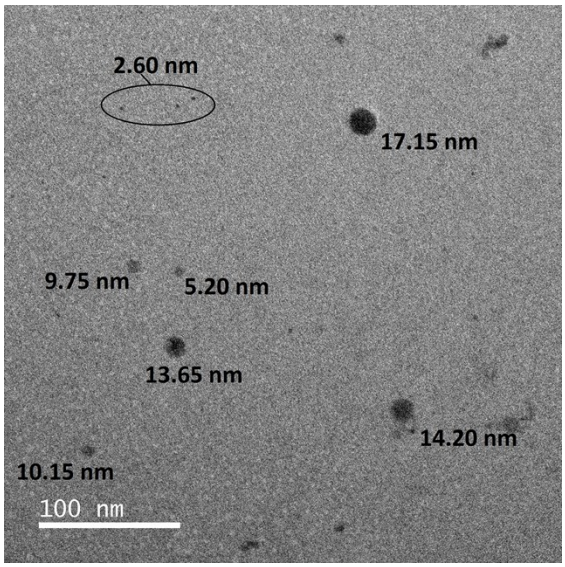

Figure S2. TEM image of the BSA-capped AgNPs measured after ~10 min of addition of NaOH. The image contains a heterogeneous distribution of particles with various sizes.

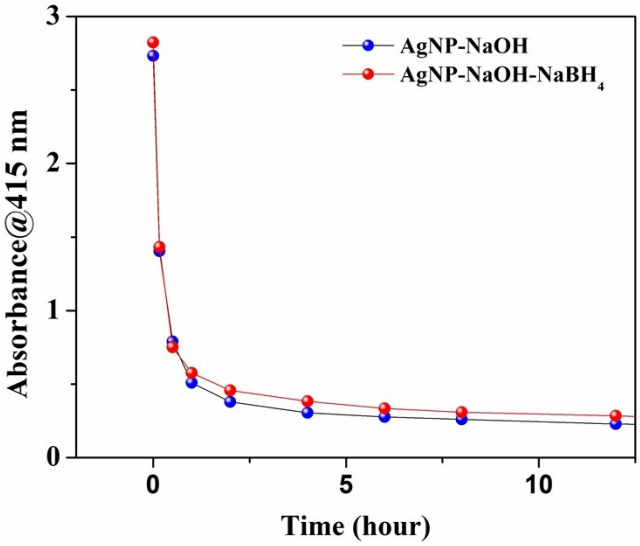

Figure S3. Time-dependent decrease of the SPR band of AgNPs (Absorbance at 415 nm) after sudden increase of the pH of the solution from 6 to 11.5 by the addition of NaOH. Blue and red spheres respectively represent the kinetic of AgNP dissolution in the absence and presence of $NaBH_4$. Both kinetics are quite similar.

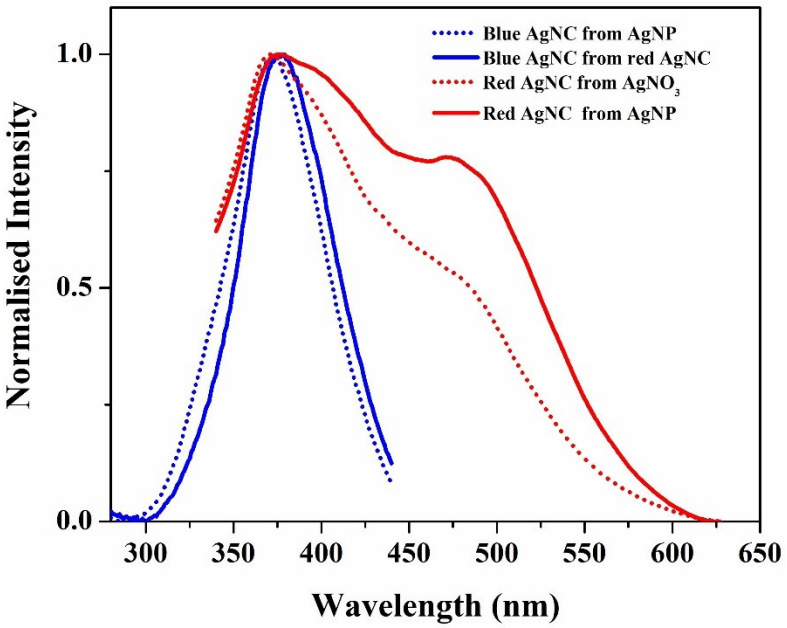

Figure S4. Excitation spectra of blue (λ_{em} = 465 nm) and red-emitting AgNCs (λ_{em} = 650 nm) synthesized from various routes. The excitation spectrum of the red-emitting AgNCs directly obtained from $AgNO_3$ is taken from ref. 37.

pH jump experiment on citrate-capped AgNPs: The citrate capped-AgNPs were synthesized by reducing silver nitrate with citrate. The citrate capped AgNP was treated with NaOH to maintain a pH of 11.50.

The citrated capped AgNP has an absorption maximum at 496 nm (Figure S5a) and on increase in pH from 7 to 11.50, there is a trivial change in absorption spectra till long hours. However, at this pH, there is a redshift in absorption maximum followed by increase in absorbance in the range 480 nm −700 nm with time. The change in the absorption spectra may be due to the aggregation of AgNPs. This was further supported by TEM image as the TEM image of citrated capped AgNPs show a uniform distribution of particle with size 7.35 ± 1.2 nm (Figure S5c) which on pH 11.50

generates aggregate structures (Figure S5d). The AgNP at higher pH is nonfluorescent in nature which indicate the absence of fluorescent AgNCs (Figure S5b).

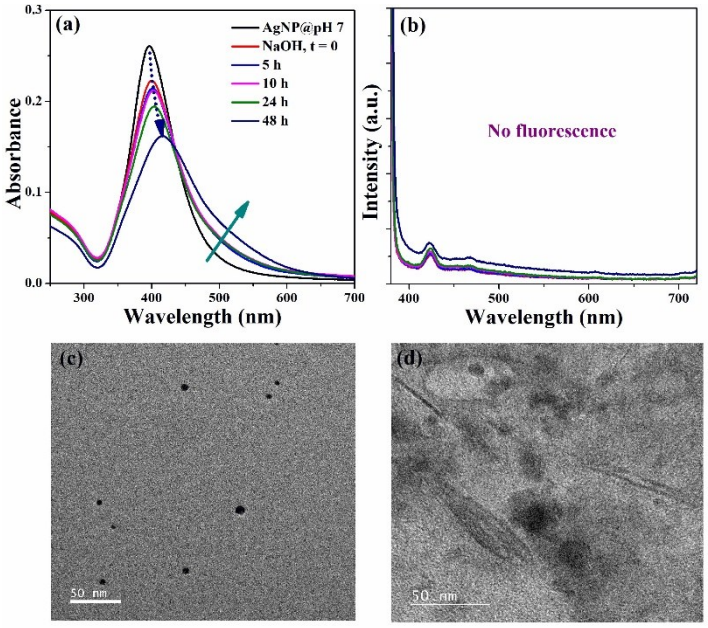

Figure S5. Time evaluation of the (a) UV-visible and (b) emission spectra (λ_{ex} = 370 nm) of citrate-capped AgNPs after enhancement of the pH from 7 to 11.5 (by addition of NaOH at t = 0). (c) and (d) are the TEM images of citrate capped AgNP at neutral and basic pH (after 48 h) respectively.

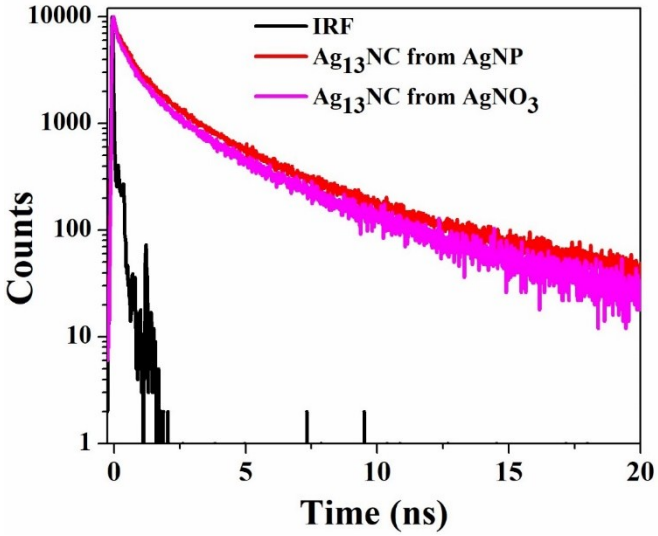

Figure S6. Comparison of fluorescence decays (λ_{ex}= 375 nm) of the red-emitting Ag_{13}NCs (λ_{em}=650 nm) obtained via two different routes: from AgNP (this work) and from $AgNO_3$ (taken from ref. 37 after adjusting the peak count).

Table S1. Fluorescence decay parameters of the red-emitting Ag_{13}NCs (λ_{ex}= 375 nm, λ_{em}=650 nm) samples obtained via two different routes. Sample A and B respectively denote red-emitting Ag_{13}NCs transformed froms AgNP (this work) and transformed directly from $AgNO_3$ (taken from ref 37)

Sample	τ_1 (a_1)/(ns)	τ_2 (a_2)/(ns)	τ_3 (a_3)/(ns)	$\langle\tau\rangle$/(ns)†
A	0.23 (0.64)	1.45 (0.29)	5.48 (0.07)	0.95
B	0.28 (0.58)	1.2 (0.35)	4.4 (0.07)	0.89

†$\langle\tau\rangle = (a_1\tau_1+a_2\tau_2+a_3\tau_3)/(a_1+a_2+a_3)$

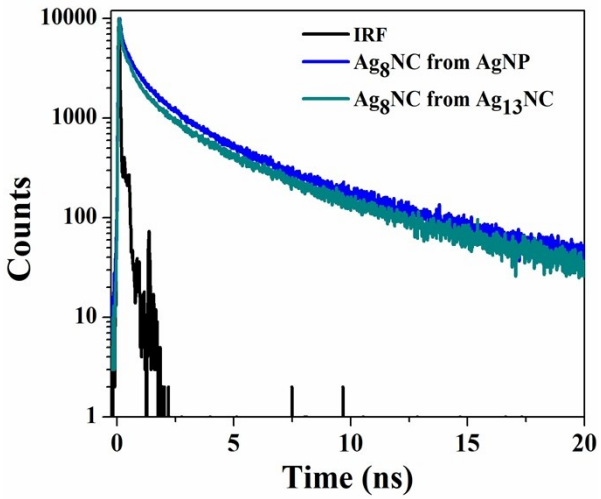

Figure S7. Fluorescence decay of the blue-emitting Ag_8NCs (λ_{ex}=375 nm and λ_{em}=465 nm) synthesized in two different routes- transformed from AgNP and via red-emitting Ag_{13}NCs.

Table S2. Fluorescence decay parameters of the blue-emitting Ag_8NCs (λ_{ex}= 375 nm, λ_{em}=465 nm) samples obtained via two different routes. Sample C and D respectively denotes Ag_8NC transforms from AgNPs and Ag_8NC transforms from red-emitting Ag_{13}NC.

Sample	τ_1 (a_1)/(ns)	τ_2 (a_2)/(ns)	τ_3 (a_3)/(ns)	τ_4 (a_4)/(ns)	<τ>/(ns)‡
C	0.075 (0.7)	0.62 (0.2)	2.85 (0.09)	9.68 (0.01)	0.53
D	0.06 (0.74)	0.5 (0.18)	2.64 (0.07)	8.84 (0.01)	0.40

‡$<\tau>= (a_1\tau_1+a_2\tau_2+a_3\tau_3+ a_4\tau_4)/(a_1+a_2+a_3+a_4)$

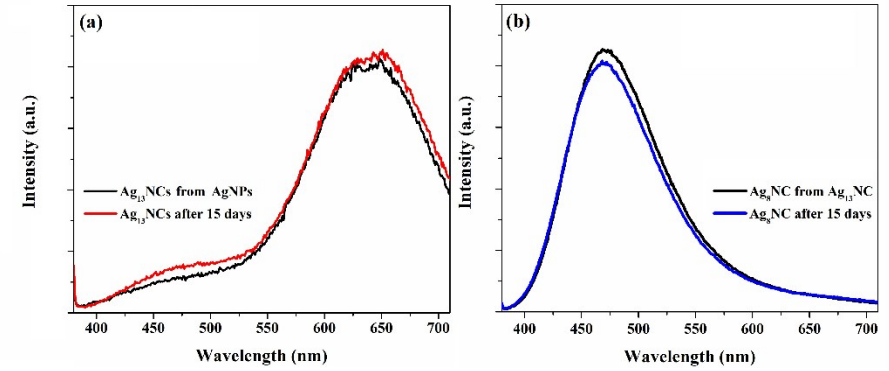

Figure S8. Fluorescence spectra of Ag_{13}NCs and Ag_8NCs stored at a low temperature (4 °C) after 15 days.

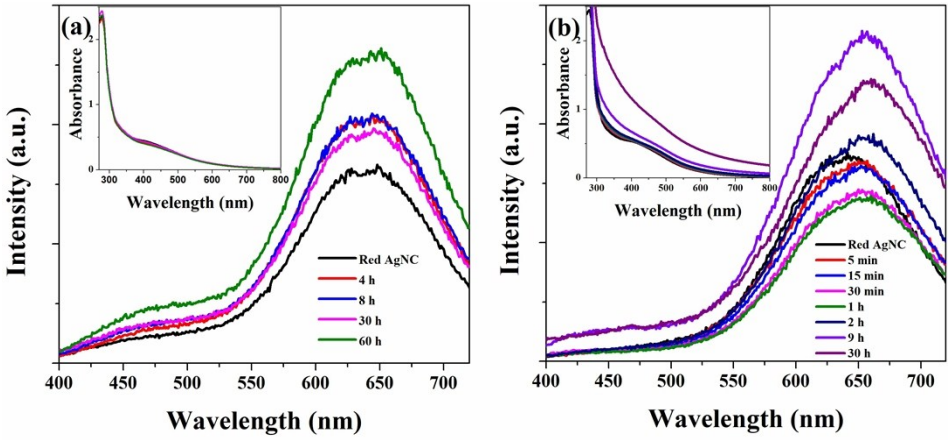

Figure S9. Emission spectra of Ag_{13}NCs samples at different times for (a) samples stored at a low temperature (4 °C) and (b) samples after acidification (pH 6) with 0.2 M HNO_3. The insets show corresponding UV-visible spectra.

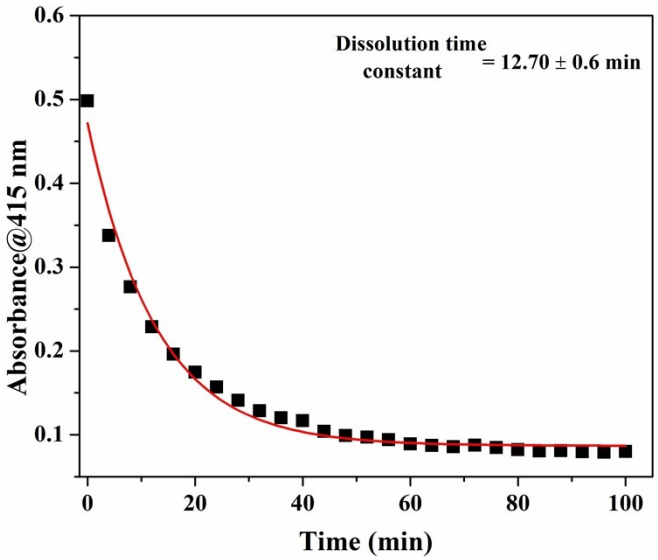

Figure S10. Dissolution kinetics of AgNP after the addition of NaOH (pH=11.50) to a 50 times diluted solution of AgNP-BSA solution. Dilution was performed to measure the absorbance more accurately than the concentrated sample.

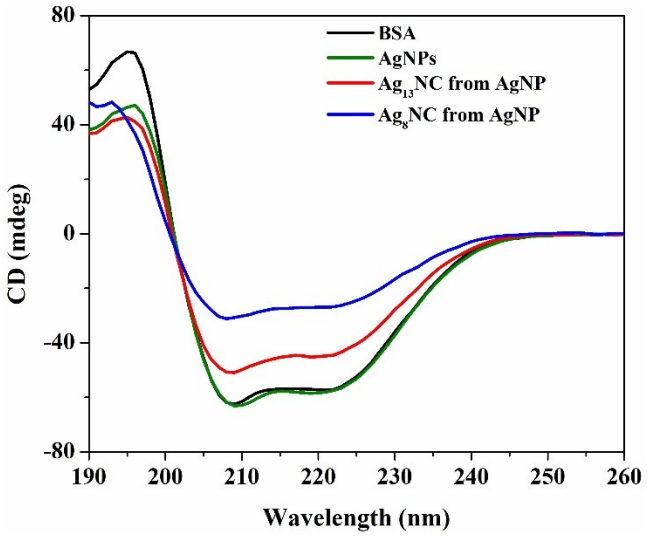

Figure S11 Circular dichroism spectra of native BSA in water, AgNP containing BSA, Ag_{13} clusters containing BSA (synthesized from AgNP) and Ag_8 clusters containing BSA (synthesized from AgNP).

Table S3. Circular dichroism data showing the helix, sheet and random coil content in native BSA in water, AgNP containing BSA, Ag_{13} clusters containing BSA (synthesized from AgNP) and Ag_8 clusters containing BSA (synthesized from AgNP).

Sample	α helix	β sheet	Random coil
BSA	0.57	0.12	0.17
AgNPs	0.56	0.15	0.16
Ag_{13}NCs	0.49	0.13	0.21
Ag_8NCs	0.31	0.20	0.28